Nadir measurements of carbon monoxide distributions by the Tropospheric Emission Spectrometer instrument onboard the Aura Spacecraft: Overview of analysis approach and examples of initial results

Curtis P. Rinsland,[1] Ming Luo,[2] Jennifer A. Logan,[3] Reinhard Beer,[2] Helen Worden,[2] Susan S. Kulawik,[2] David Rider,[2] Greg Osterman,[2] Michael Gunson,[2] Annmarie Eldering,[2] Aaron Goldman,[4] Mark Shephard,[5] Shepard A. Clough,[5] Clive Rodgers,[6] Michael Lampel,[7] and Linda Chiou[8]

Received 25 May 2006; revised 29 September 2006; accepted 12 October 2006; published 22 November 2006.

[1] We provide an overview of the nadir measurements of carbon monoxide (CO) obtained thus far by the Tropospheric Emission Spectrometer (TES). The instrument is a high resolution array Fourier transform spectrometer designed to measure infrared spectral radiances from low Earth orbit. It is one of four instruments successfully launched onboard the Aura platform into a sun synchronous orbit at an altitude of 705 km on July 15, 2004 from Vandenberg Air Force Base, California. Nadir spectra are recorded at 0.06-cm^{-1} spectral resolution with a nadir footprint of 5 × 8 km. We describe the TES retrieval approach for the analysis of the nadir measurements, report averaging kernels for typical tropical and polar ocean locations, characterize random and systematic errors for those locations, and describe instrument performance changes in the CO spectral region as a function of time. Sample maps of retrieved CO for the middle and upper troposphere from global surveys during December 2005 and April 2006 highlight the potential of the results for measurement and tracking of global pollution and determining air quality from space. **Citation:** Rinsland, C. P., et al. (2006), Nadir measurements of carbon monoxide distributions by the Tropospheric Emission Spectrometer instrument onboard the Aura Spacecraft: Overview of analysis approach and examples of initial results, *Geophys. Res. Lett.*, *33*, L22806, doi:10.1029/2006GL027000.

1. Introduction

[2] Carbon monoxide (CO) is a by-product of incomplete combustion of fossil fuels and biomass, and is produced by oxidation of methane (CH_4) and other hydrocarbons. Combustion of fossil fuels is the main source of CO at northern mid-latitudes, while biomass burning (in the local dry season), biomass fuel, and oxidation of isoprene are important sources in the tropics. Oxidation of methane provides a relatively uniform background of CO. Reaction with the hydroxyl radical (OH) is the main removal process for CO [*Levy*, 1971], and reaction with OH is the dominant path for removal of many atmospheric species. Oxidation of CO and methane provides the major source of tropospheric ozone [e.g., *Logan et al.*, 1981]. The lifetime of CO is several weeks and hence CO is a useful tracer of atmospheric transport.

[3] Space-based tropospheric CO distributions retrieved from nadir measurements were first obtained from the U.S. shuttle by the MAPS (Measurement of Air Pollution from Satellites) experiment during four flights (November 1981, October 1984, April 1994, and October 1994) at latitudes between 57°N to 58°S [*Reichle and Connors*, 1999]. The gas filter radiometer operated in the (1-0) band region at 4.7 μm with maximum sensitivity in the middle-upper troposphere [*Pougatchev et al.*, 1998]. More recently, global space-based nadir measurements of CO have been obtained with the MOPITT (Measurements of Air Pollution from Satellites) instrument on the Terra spacecraft [*Edwards et al.*, 2004], Interferometric Monitor of Greenhouse Gases (IMG) [*Barret et al.*, 2005], the Tropospheric Emission Spectrometer (TES) on the Aura spacecraft [*Beer et al.*, 2001], the Atmospheric Infrared Sounder (AIRS) launched on the Aqua satellite [*Aumann et al.*, 2003], and the Scanning Imaging Spectrometer for CHartographY (SCIAMACHY) UV-visible-near-IR spectrometer [*Bovensmann et al.*, 1999]. Limb CO observations are obtained in solar occultation mode by the Atmospheric Chemistry Experiment (ACE) [*Bernath et al.*, 2005] and in emission by the Microwave Limb Sounder (MLS) on Aura [*Filipiak et al.*, 2005]. The purpose of this paper is to provide an overview of early TES nadir CO measurements. We describe the approach used for the TES nadir retrievals, document the selections of spectral windows, provide averaging kernels for mid-latitude and polar conditions, report an error evaluation for those sample locations, and describe changes in TES instrument performance in the CO spectral region since launch. Carbon monoxide and ozone are two of the five main pollutants monitored by the U.S. Environmental Protection Agency

[1]NASA Langley Research Center, Hampton, Virginia, USA.
[2]Jet Propulsion Laboratory, California Institute of Technology, Pasadena, California, USA.
[3]Division of Engineering and Applied Sciences, Harvard University, Cambridge, Massachusetts, USA.
[4]Department of Physics, University of Denver, Denver, Colorado, USA.
[5]Atmospheric and Environmental Research, Inc., Lexington, Massachusetts, USA.
[6]Clarendon Laboratory, Oxford University, Oxford, UK.
[7]Raytheon Company, Pasadena, California, USA.
[8]Science Applications International Corporation, Hampton, Virginia, USA.

0094-8276/06/2006GL027000$05.00

(EPA) and are now measured globally and simultaneously by the TES instrument.

2. TES Fourier Transform Spectrometer

[4] TES is an infrared imaging Fourier Transform Spectrometer (FTS) operating in the spectral range 650–3050 cm^{-1} (3.3–15.4 μm) [*Beer et al.*, 2001]. The Connes-type four port FTS has 16 spatial pixels in each of four optically conjugated mercury cadmium telluride focal plane arrays, each optimized for a different spectral region and operating at a temperature of 64 K using mechanical refrigerators. In addition, each focal plane is equipped with interchangeable cooled filters that limit the instantaneous spectral bandwidths to about 250 cm^{-1}. This provides needed control over the instrument thermal background and reduces the data rate. Except for two external mirrors (part of the pointing system), the entire optical path is radiatively-cooled to about 180 K, to further reduce the instrument background. The nadir foot print is 5 × 8 km, where the 16-pixel (5 × 0.5 km) average measurements are used in the retrievals. The nadir foot print for TES is similar to that of MOPITT and AIRS. TES is a unique spaceborne FTS in that it can observe high resolution infrared thermal emission in both nadir and limb modes and can point anywhere within 45° of nadir (cross track and in track) [*Beer et al.*, 2001].

[5] TES has several operating modes for nadir observations [*Beer et al.*, 2001]. Key modes for nadir observations are stare, transect, and step and stare modes. The stare mode allows TES to point a ground target for several minutes. The transect mode point at a set of contiguous footprint-size areas within 45 degrees of the instrument nadir angle. The step and stare mode point at the nadir location for a single scan and can be repeated indefinitely. The global survey mode of 16 orbits of nadir and limb observations repeated every other day. Routine limb observations were discontinued in April 2005 to extend instrument lifetime with no significant impact on CO. There was limited ability of the limb measurements to sample source regions over those long paths.

3. TES CO Measurements

[6] Spectral windows for the retrieval of CO were selected based on sensitivities calculated for TES filter 1A1 (1890–2260 cm^{-1}) where the CO (1-0) band is located [*Worden et al.*, 2004]. TES nadir measurements are recorded at 0.06-cm^{-1} spectral resolution (8.33 cm maximum optical path difference derived from double-sided interferograms) with a forward model that includes a model for the water vapor continuum with a climatological CO_2 mixing ratio profile [*Clough et al.*, 2006]. The TES retrieval algorithm estimates an atmospheric profile by simultaneously minimizing the difference between observed and model spectral radiances subject to the constraint that the solution is consistent with an a priori mixing ratio profile within covariance constraints [*Bowman et al.*, 2006; *Kulawik et al.*, 2006a].

[7] Spectroscopic parameters were taken from the 2000 HITRAN database with updates through September 2001 [*Rothman et al.*, 2003], though further updates from HITRAN 2004 [*Rothman et al.*, 2005] have been incorporated and are used in the forward model calculations and analysis. Similar to most other experiments operating in the infrared [e.g., *Boone et al.*, 2005], TES uses spectral windows to limit the impact of spectroscopic errors in the retrievals from 11 windows between 2086.06 and 2176.66 cm^{-1}. Temperature and interferences fitted for all windows are N_2O, CO_2, O_3, and H_2O. Carbon monoxide profiles are retrieved after temperature, ozone, and water vapor profiles are fitted in addition to the interferences.

[8] Measured radiances are compared with those calculated for the same location with the TES forward model. The measured radiances are apodized with Norton-Beer strong apodization [*Norton and Beer*, 1976]. As clouds are ubiquitous in the atmosphere and substantially affect the radiances measured by TES, an algorithm is used to quantify how clouds impact the measured optical depths in the spectral windows selected for retrieving temperature and gas constituent profiles [*Kulawik et al.*, 2006b; *Bowman et al.*, 2006]. The approach is to retrieve a single layer, frequency-dependent cloud with an effective height, a Gaussian profile in altitude, and effective cloud thickness. No scattering is assumed. This approach makes possible the retrieval and error characterization of atmospheric parameters including CO, temperature, water vapor, and ozone characterized in the presence of clouds based on the optimal estimation technique [*Rodgers*, 2000]. Characterization of TES retrieval information content includes the quantification of smoothing, ''cross-state'', and systematic errors [*Bowman et al.*, 2006, Figure 5]. All parameters are derived from a simultaneous analysis of the measured spectrum. Although error in the temperature retrieval propagates into the error for CO, it is small compared the other sources of error.

[9] A key factor for TES CO results has been the impact of changes in instrument alignment as a function of time. Figure 1 displays the normalized integrated spectral magnitude (ISM) (top panel), beam splitter temperature (middle panel), and DOF for latitudes of 30°N–30°S as a function of time. The ISM is a sensitive indicator of signal levels at the TES detectors and is calculated by integrating a spectrum over wave number. It is the primary quantity used to quantify and detect trends in the TES instrument alignment and performance. An overall trend of declining ISM with time and the measured beam splitter temperature is apparent, with increases in beam splitter temperatures when the detectors are de-iced periodically. Warm up of the optical bench on November 29-December 2, 2005 improved the TES beam splitter alignment, with an integrated spectral magnitude increase for the 1A1 filter of a factor of 3.4 as compared to the pre-warm up value. The TES averaging kernel matrix was used to compute the DOF (degrees of freedom) for signal of the retrieval [*Worden et al.*, 2004]. The DOF may be interpreted as the number of statistically independent elements of the retrieval [*Rodgers*, 2000; *Bowman et al.*, 2006] with a DOF for signal of 0.8 for TES CO predicted prior to launch [*Worden et al.*, 2004]. Shortly after launch, the measured DOF for TES CO signal typically varied from 0.5–1.5, high in tropics with values up to two and gradually dropping below 0.5 at high latitudes. As the signal strength of 1A1 filter became weaker from end of 2004 to November 2005, the DOF for TES CO gradually declined. The optical bench warm up improved

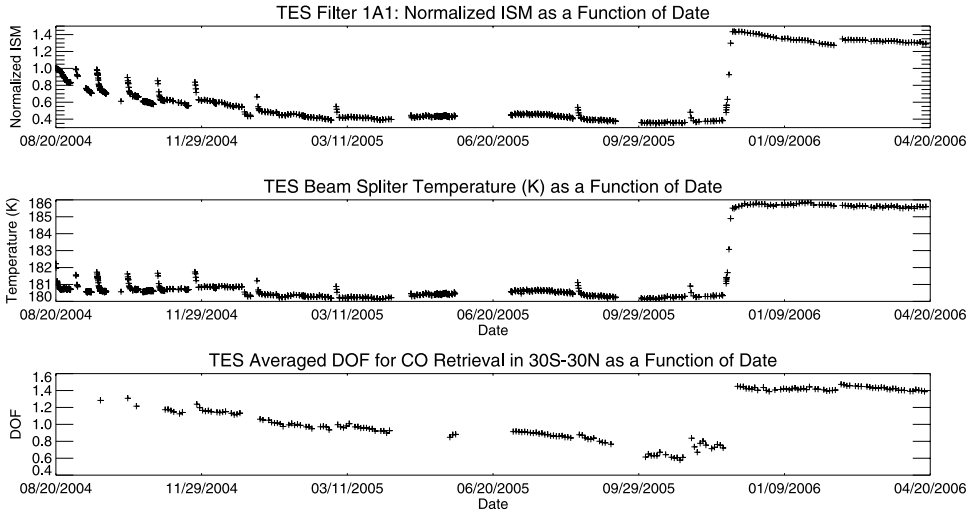

Figure 1. (top) Time series of measured normalized Integrated Spectral Magnitude (ISM), (middle) beam splitter temperature, and (bottom) average DOF for 30°N–30°S latitude. The ISM is normalized to 1.0 at the beginning of the time series. The results were derived from TES Level 1A R7/R8 data.

TES signal to noise ratios so the DOF for CO increased to an averaged value of 1.45 (from the pre-warm-up value of 0.72) with many values now greater than 2.0 at 30°S–30°N.

[10] Figure 2 displays sample TES volume mixing ratio retrievals, averaging kernels, and evaluations of random and smoothing errors for tropical and polar conditions from early TES measurements when the ISM was high. TES data consists of profiles of CO reported at 24 levels per pressure decade (e.g., 1000 hPa to 100 hPa) between the surface and 100 hPa (~16 km). The fine vertical grid is necessary to accurately model variations of temperature, water vapor, ozone, clouds and molecular interferences in the atmosphere. TES averaging kernels are reported for each retrieved profile. Selected pressure levels show that the sensitivity is lowest at the surface and increases with altitude with a maximum in the free troposphere for both

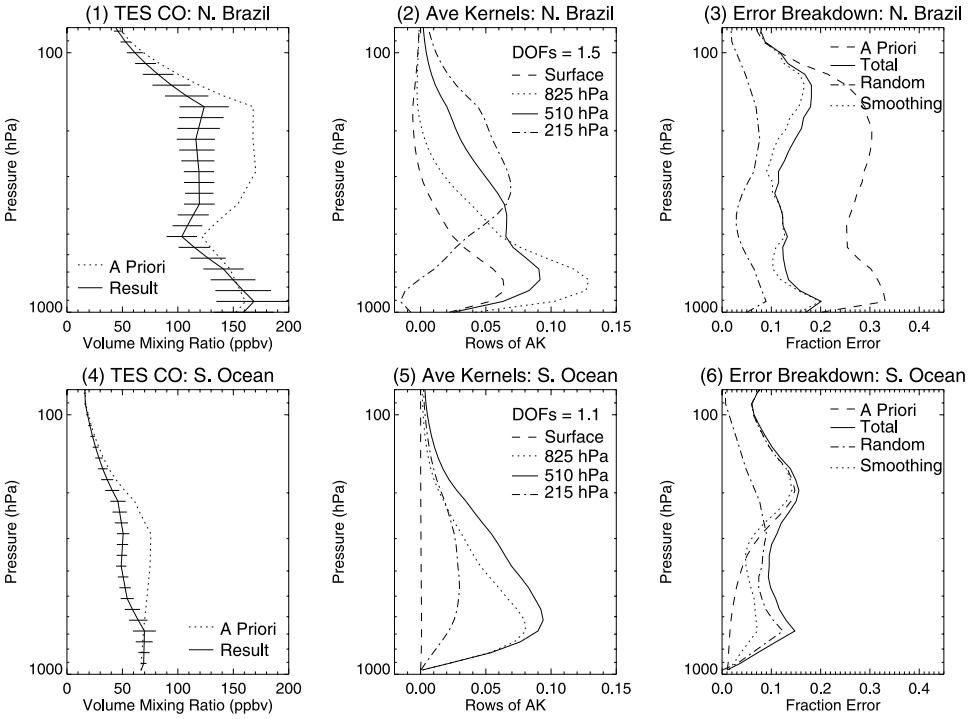

Figure 2. Sample carbon monoxide retrieval, averaging kernels, random and systematic error estimates as a function of pressure for tropical and polar latitudes. The tropical occultation was recorded over northern Brazil (latitude 3.9°S, longitude 58.6°W). The lower panels correspond to a southern polar ocean scene at 58°S, 81°E. Horizontal error bars show total errors. DOFs are reported for both example cases. Results were derived from TES V001 data from measurements on September 20, 2004.

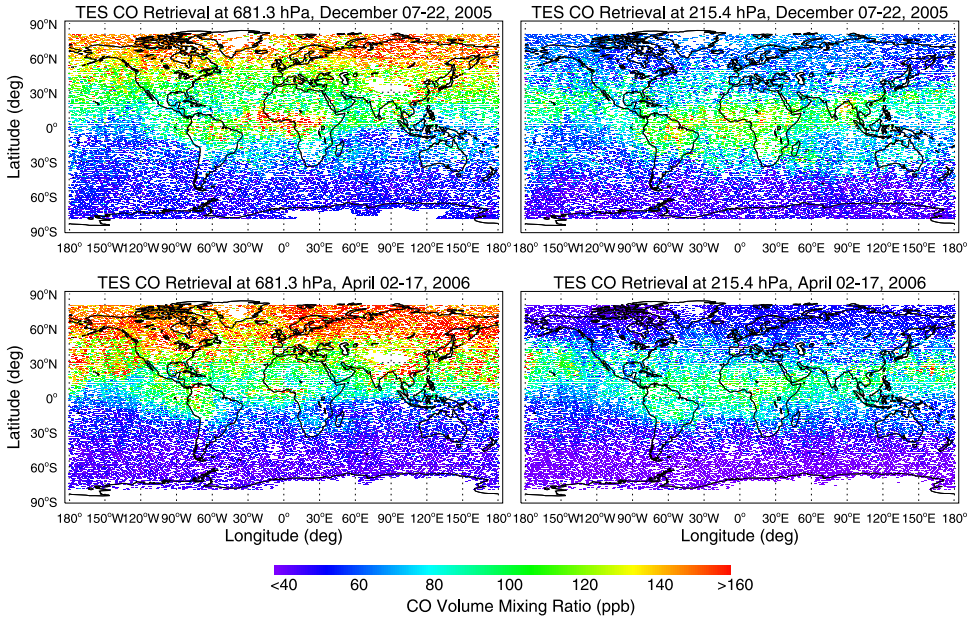

Figure 3. Global maps of CO volume mixing ratio distributions at 215.4 hPa and 681.3 hPa from TES 16-day global surveys from December 2005 and April 2006. Maps are from TES V002 measurements recorded after the optical bench warm-up.

tropical and polar regions. Similar to MOPITT, TES profile data are highly correlated, with about 1–2 pieces of independent vertical information for each sounding. Random error due to instrument noise with a value of ~10% is lower than the smoothing error in most places. Systematic error due to errors in the HITRAN spectroscopic parameters [*Rothman et al.*, 2005] and the cross-state error terms are small components in the error budget. The smoothing error is the largest component (~20%), with the total relative error (~20–30%) combined from the random, the smoothing, the systematic, and the cross-state errors [*Bowman et al.*, 2006].

[11] The current TES CO retrievals assume a priori profiles given by the MOZART chemical transport model first described by *Brasseur et al.* [1998]. Monthly mean mixing ratios in 10° latitude by 60° longitude bins are used to create the a priori profiles assumed for TES retrievals with an altitude-dependent Tikhonov constraint [*Kulawik et al.*, 2006a]. In the case of the southern polar region in Figure 2, the total retrieval error is greater than the a priori error due to the use of the model data as a priori. In contrast, the MOPITT analysis relies on a single a priori profile and covariance matrix for CO retrievals [*Deeter et al.*, 2003, 2004]. Near complete global coverage is achieved in 3 days [see *Liu et al.*, 2006, for an example of a recent MOPITT study]. There are significant differences in the a priori profile and covariance matrix constraints for TES retrievals and those adopted by MOPITT for their analysis. The influence of the differences in a priori constraints to the retrievals have been described and characterized (M. Luo et al., Comparison of carbon monoxide measurements by TES and MOPITT: The influence of a priori data and instrument characteristics on nadir atmospheric species retrievals, submitted to *Journal of Geophysical Research*, 2006, hereinafter referred to as Luo et al., submitted manuscript, 2006).

[12] Figure 3 displays CO mixing ratio retrieved from TES global surveys during two week time periods at lower and upper tropospheric pressure levels during December 2005 and April 2006. Data quality screening is done following TES Level 2 Data User's Guide (G. Osterman et al., TES level 2 data user's guide, Jet Propul. Lab., Pasadena, Calif., available at http://tes.jpl.nasa.gov/docsLinks/documents.cfm, 2006). The CO mixing ratios in the two time periods show interhemispheric gradient in the lower troposphere with higher mixing ratios measured in the northern hemisphere than in the southern hemisphere. The December 2005 measurements at 681.1 hPa show elevated CO from biomass burning over western Africa extending into the Atlantic. The upper tropospheric CO distributions show the evidence of the latitude/longitude binned a priori described above, indicating the influence of the a priori in the retrievals where DOF are less than one (Luo et al., submitted manuscript, 2006). Fields for April 2006 CO are dominated by urban pollutions in the northern hemisphere. Figure 4 further illustrates the variability in TES observed CO mixing ratio during a few days of April. For example, the measurements show CO pollution sources over China (southern or northern city areas, e.g., Beijing or Shanghai areas) and their downwind plumes over Pacific Ocean are captured by TES. These CO sources or plumes at 681 hPa are detected as high as 280 ppbv.

4. Summary and Conclusions

[13] Analysis procedures, spectral windows selections, average kernels, and an analysis of random and systematic sources of error have been reported for TES CO. Changes in instrument performance of the TES CO nadir measurements have been described with examples presented illustrating the capability of TES to provide bi-weekly global maps of CO distributions with 0.5–2 statistically independent tro-

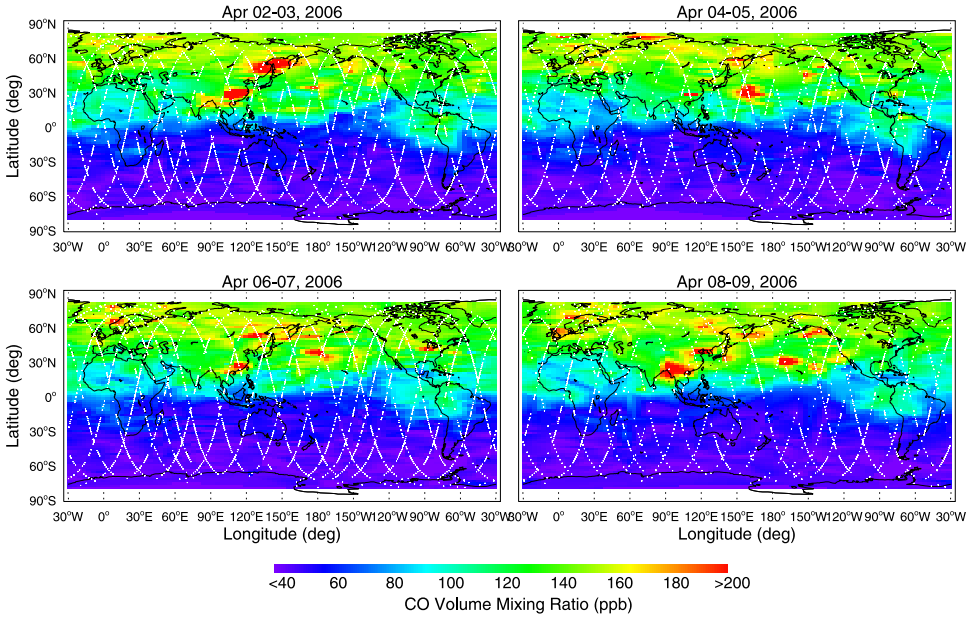

Figure 4. Interpolated TES Global Survey CO data at 681.3 hPA from April 2006. The orbital track shows the locations of the TES measurements.

pospheric degrees of freedom. Space-based tropospheric CO profile measurements from TES are now being compared with those by ACE, MOPITT, MLS, AIRS, and SCIAMACHY in addition to measurements from aircraft missions. Additional comparisons of TES profiles with those of other sensors will extend those planned for CO and other TES products [*Osterman et al.*, 2005].

[14] The TES optical bench warm up activity in early December 2005 has significantly increased the sensitivity of the TES instrument with results indicating more than a factor of 3 sensitivity improvement in the CO measurement spectral region. The higher CO sensitivity (both vertical resolution and signal-to-noise) in combination with co-located measurements of O_3 will increase the capability of TES to measure global air quality and to assess the relative roles of photochemistry and transport in key regions such as over the U.S., Asia, and Europe. This work provides a quantitative assessment of the capability of the TES instrument to measure tropospheric CO profiles since Aura launch and provides recent examples of TES maps of CO pollution to highlight the improved capability of the instrument and the availability of the data for air quality and tropospheric chemistry studies.

[15] **Acknowledgments.** Research at the Jet Propulsion Laboratory described in this paper was performed under contract with the National Aeronautics and Space Administration. Curtis Rinsland participates as a science team member and unfunded coinvestigator.

References

Aumann, H. H., et al. (2003), AIRS/AMSU/HSB on the aqua mission: Design, science objectives, data products, and processing systems, *IEEE Trans. Geosci. Remote Sens.*, *41*, 253–264.

Barret, B., et al. (2005), Global carbon monoxide vertical distributions from spaceborne high-resolution FTIR nadir measurements, *Atmos. Chem. Phys. Disc.*, *5*, 4599–4639.

Beer, R., T. A. Glavich, and D. M. Rider (2001), Tropospheric emission spectrometer for the Earth Observing Systems Aura satellite, *Appl. Opt.*, *40*, 2356–2367.

Bernath, P. F., et al. (2005), Atmospheric Chemistry Experiment (ACE): Mission overview, *Geophys. Res. Lett.*, *32*, L15S01, doi:10.1029/2005GL022386.

Boone, C. D., et al. (2005), Retrievals for the atmospheric chemistry experiment fourier transform spectrometer, *Appl. Opt.*, *44*, 7218–7231.

Bovensmann, H., J. P. Burrows, M. Buchwitz, J. Frerick, S. Noël, V. V. Rozanov, K. V. Chance, and A. P. H. Goede (1999), SCIAMACHY: Mission objectives and measurement modes, *J. Atmos. Sci.*, *56*, 125–150.

Bowman, K. W., et al. (2006), Tropospheric emission spectrometer: Retrieval method and error analysis, *IEEE Trans. Geosci. Remote Sens.*, *44*, 1297–1307.

Brasseur, G. P., D. A. Hauglustaine, S. Walters, P. J. Rasch, J.-F. Müller, C. Granier, and X. X. Tie (1998), MOZART, a global chemical transport model for ozone and related chemical tracers: 1. Model description, *J. Geophys. Res.*, *103*, 28,265–28,290.

Clough, S. A., et al. (2006), Forward model and Jacobians for tropospheric emission spectrometer retrievals, *IEEE Trans. Geosci. Remote Sens.*, *44*, 1308–1323.

Deeter, M. N., et al. (2003), Operational carbon monoxide retrieval algorithm and selected results for the MOPITT instrument, *J. Geophys. Res.*, *108*(D14), 4399, doi:10.1029/2002JD003186.

Deeter, M. N., L. K. Emmons, D. P. Edwards, J. C. Gille, and J. R. Drummond (2004), Vertical resolution and information content of CO profiles retrieved by MOPITT, *Geophys. Res. Lett.*, *31*, L15112, doi:10.1029/2004GL020235.

Edwards, D. P., et al. (2004), Observations of carbon monoxide and aerosols from the Terra satellite: Northern Hemisphere variability, *J. Geophys. Res.*, *109*, D24202, doi:10.1029/2004JD004727.

Filipiak, M. J., R. S. Harwood, J. H. Jiang, Q. Li, N. J. Livesey, G. L. Manney, W. G. Read, M. J. Schwartz, J. W. Waters, and D. L. Wu (2005), Carbon monoxide measured by the EOS Microwave Limb Sounder on Aura: First results, *Geophys. Res. Lett.*, *32*, L14825, doi:10.1029/2005GL022765.

Kulawik, S. S., et al. (2006a), Calculation of altitude-dependent Tikhonov constraints for TES nadir retrievals, *IEEE Trans. Geosci. Remote Sens.*, *44*, 1334–1342.

Kulawik, S. S., et al. (2006b), Implementation of cloud retrievals for Tropospheric Emission Spectrometer (TES) atmospheric retrievals: 1. Description and characterization of errors on trace gas retrievals, *J. Geophys. Res.*, doi:10.1029/2005JD006733, in press.

Levy, H., II. (1971), Normal atmosphere: Large radical and formaldehyde concentrations predicted, *Science*, *173*, 141–143.

Liu, J., J. R. Drummond, D. B. A. Jones, Z. Cao, H. Bremer, J. Kar, J. Zou, F. Nichitiu, and J. C. Gille (2006), Large horizontal gradients in atmospheric CO at the synoptic scale as seen by spaceborne measurements of pollution in the troposphere, *J. Geophys. Res.*, *111*, D02306, doi:10.1029/2005JD006076.

Logan, J. A., M. J. Prather, S. C. Wofsy, and M. B. McElroy (1981), Tropospheric chemistry: A global perspective, *J. Geophys. Res.*, *86*, 7210–7254.

Norton, R., and R. Beer (1976), New apodizing functions for Fourier spectrometry, *J. Opt. Soc. Am.*, *66*, 259–264.

Osterman, G., et al. (2005), Tropospheric Emission Spectrometer (TES) validation report version 1.00, *JPL D33192*, Jet Propul. Lab., Pasadena, Calif. (Available at http://tes.jpl.nasa.gov/docsLinks/documents.cfm)

Pougatchev, N. S., et al. (1998), Ground-based infrared solar spectroscopic measurements of carbon monoxide during 1994 Measurement of Air Pollution From Space Flights, *J. Geophys. Res.*, *103*, 19,317–19,325.

Reichle, H. G., Jr., and V. S. Connors (1999), The mass of CO in the atmosphere during October 1984, April 1994, and October 1994, *J. Atmos. Sci.*, *56*, 307–310.

Rodgers, C. D. (2000), *Inverse Methods for Atmospheric Sounding: Theory and Practice*, World Sci., Hackensack, N. J.

Rothman, L. S., et al. (2003), The HITRAN molecular spectroscopic database: Edition of 2000 including updates through 2001, *J. Quant. Spectrosc. Radiat. Transfer*, *82*, 5–44.

Rothman, L. S., et al. (2005), The HITRAN 2004 molecular spectroscopy database, *J. Quant. Spectrosc. Radiat. Transfer*, *96*, 139–204.

Worden, J., S. S. Kulawik, M. W. Shephard, S. A. Clough, H. Worden, K. Bowman, and A. Goldman (2004), Predicted errors of tropospheric emission spectrometer nadir retrievals from spectral window selection, *J. Geophys. Res.*, *109*, D09308, doi:10.1029/2004JD004522.

R. Beer, A. Eldering, M. Gunson, S. S. Kulawik, M. Luo, G. Osterman, D. Rider, and H. Worden, Jet Propulsion Laboratory, California Institute of Technology, 4800 Oak Grove Drive, Pasadena, CA 91109, USA.

L. Chiou, Science Applications International Corporation, 1 Enterprise Parkway, Mail Stop 927, Hampton, VA 23666, USA.

S. A. Clough and M. Shephard, AER, Inc., 131 Hartwell Avenue, Lexington, MA 02421, USA.

A. Goldman, Department of Physics and Astronomy, University of Denver, P.O. Box 3000, Denver, CO 80208, USA.

M. C. Lampel, Raytheon Company, 299 North Euclid Avenue, Suite 500, Pasadena, CA 91101, USA.

J. Logan, Division of Engineering and Applied Sciences, Harvard University, 29 Oxford Street, Cambridge, MA 02138, USA.

C. P. Rinsland, NASA Langley Research Center, Mail Stop 401A, Hampton, VA 23681-2199, USA. (c.p.rinsland@larc.nasa.gov)

C. Rodgers, Clarendon Laboratory, Oxford University, Parks Road, Oxford OX1 3PU, UK.